Theory of boron-vacancy complexes in silicon

J. Adey, R. Jones, and D. W. Palmer
School of Physics, University of Exeter, Exeter EX4 4QL, United Kingdom

P. R. Briddon
Physics Centre, School of Natural Science, Newcastle upon Tyne NE1 7RU, United Kingdom

S. Öberg
Department of Mathematics, Luleå University of Technology, SE-97187 Luleå, Sweden
(Received 5 November 2004; published 26 April 2005)

The substitutional boron-vacancy B_sV complex in silicon is investigated using the local density functional theory. These theoretical results give an explanation of the experimentally reported, well established metastability of the boron-related defect observed in *p*-type silicon irradiated at low temperature and of the two hole transitions that are observed to be associated with one of the configurations of the metastable defect. B_sV is found to have several stable configurations, depending on charge state. In the positive charge state the second nearest neighbor configuration with C_1 symmetry is almost degenerate with the second nearest neighbor configuration that has C_{1h} symmetry since the bond reconstruction is weakened by the removal of electrons from the center. A third nearest neighbor configuration of B_sV has the lowest energy in the negative charge state. An assignment of the three energy levels associated with B_sV is made. The experimentally observed $E_v+0.31$ eV and $E_v+0.37$ eV levels are related to the donor levels of second nearest neighbor B_sV with C_1 and C_{1h} symmetry respectively. The observed $E_v+0.11$ eV level is assigned to the vertical donor level of the third nearest neighbor configuration. The boron-divacancy complex B_sV_2 is also studied and is found to be stable with a binding energy between V_2 and B_s of around 0.2 eV. Its energy levels lie close to those of the V_2. However, the defect is likely to be an important defect only in heavily doped material.

DOI: 10.1103/PhysRevB.71.165211 PACS number(s): 61.72.Bb, 61.72.Ji, 61.72.Tt, 71.15.Nc

I. INTRODUCTION

In recent years there has been much interest in the defects formed by the interaction with dopants of self-interstitials, one of the primary damage products of electron irradiation and ion implantation. In the case of boron this interest has stemmed largely from the need to explain and model the phenomena of transient enhanced diffusion where the diffusion of boron is increased due to the supersaturation of self-interstitials and electrically inactive boron-interstitial clusters are formed.[1] This has meant that, to our knowledge, no other *ab initio* studies have been undertaken that consider the interaction of the dopant boron with the other primary damage product, namely the vacancy. Although the substitutional-boron-vacancy, B_sV, center is unstable at room temperature,[2] we will show here that BV_2 complexes enjoy greater stability.

Vacancies are readily introduced into boron-doped Si by irradiation and become mobile around 180 K. They then complex primarily with boron. The boron-vacancy (B_sV) defect in silicon was first investigated using electron paramagnetic resonance (EPR) and assigned to the Si-*G*10 EPR center.[2] Later, further information on the hyperfine interactions with surrounding shells of silicon atoms was obtained by electron-nuclear double resonance (ENDOR).[3] The model deduced from EPR studies is shown in Fig. 1(*i*), where a reconstruction occurs between the dangling bonds of one pair of silicon atoms, labeled *b* and *c*, lowering the symmetry to C_1. For lightly irradiated *p*-type material, the complex is visible in EPR only under photoillumination, and is detected directly in heavily irradiated material only when the Fermi level moves deeper into the gap. The center is unique among vacancy-impurity centers, owing to its triclinic symmetry and having a structure where the boron atom lies outside the vacancy cage. It anneals around 260 K.[2] The hyperfine structure in *G*10 demonstrates that 55% of the spin density lies on one Si atom labeled *d* in Fig. 1 with a substantial fraction (87%) of *p* component. There is an alternative reconstruction possible between atoms *b* and *d* which would result in an equivalent defect. At low temperatures, the defect is trapped in one of these states but between 30 and 80 K it is able to switch to the other electronic configuration, surmounting a barrier of 0.044 eV.[2] Deep level transient spectroscopic (DLTS) studies on *e*-irradiated boron-doped Si which has been annealed to 150–200 K when vacancies become mobile, reveal three levels at $E_v+0.31$, $E_v+0.37$, and $E_v+0.11$ eV thought to be associated with B_sV.[4–6] From published data,[4–7] we assess the hole-capture cross sections to be about $6-10\times10^{-16}$ cm^2, $1-5\times10^{-17}$ cm^2 and about 4×10^{-16} cm^2 for the $E_v+0.31$, $E_v+0.37$, and $E_v+0.11$ eV levels, respectively.

The large cross-section value for the $E_v+0.31$ eV level might indicate that this is a $(-/0)$ level in contrast with a $(0/+)$ transition assigned to $E_v+0.37$ eV. However, this would imply a negative-*U* behavior and an unstable neutral defect. Clearly, this is inconsistent with the observation of a stable Si-*G*10 EPR spin-1/2 center in heavily irradiated material.[2] We thus conclude that both $E_v+0.31$ and $E_v+0.37$ are $(0/+)$ donor levels.

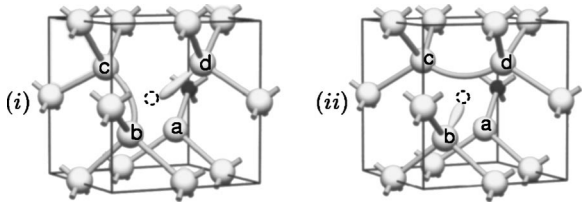

FIG. 1. The boron-vacancy defect, in the second nearest neighbor configuration with C_1 symmetry [structure (i)], as proposed by Watkins (see Ref. 2). We label this, and the equivalent one where the reconstructed bond lies between atoms *b* and *d*, $2nn(C_1)$. The C_{1h} form [structure (ii)] labeled $2nn(C_{1h})$ differs from the $2nn(C_1)$ configuration by having a reconstructed bond between atoms *c* and *d*. The black ball represents the boron atom and atoms *a*, *b*, *c*, and *d* are the neighbors to the vacancy which is shown as a dashed ring to aid the reader.

The $E_v+0.11$ eV level is seen by DLTS when the sample is heated at 220 K for 30 min under reverse bias followed by quenching to 80 or 40 K.[4–6] The other pair is detected after cooling under zero or forward bias and since this pair of levels always give the same amplitude ratio, they were attributed to the same atomic configuration (labeled *A*).[4] The third level, at $E_v+0.11$ eV, is due to a different configuration labeled *B*. Configuration *B* can be converted back to *A* again by a second anneal, this time under zero bias. This suggests a charge-driven bistability between configurations *A* and *B* where configuration *A* is stable in the more positive charge state. Since the Si-*G*10 EPR center is detected in material cooled in the same way as the DLTS experiments, i.e., at zero bias, the *A* configuration must correspond to the positive charge state which becomes EPR active following photoillumination or when the Fermi level rises above $E_v+0.31$ or $E_v+0.37$ eV.

Chantre[8] introduced boron related centers by quenching laser-annealed silicon doped with boron at 1300 °C. He found two levels, one at $E_v+0.50$ eV (H_1) and the other at $E_v+0.36$ eV (H_2), which were stable to about 300 K. The levels are associated with a bistable defect in which configuration Q_1 is stable for the positively charged center and Q_2 stable for the neutral center. These transform into each other around 270 K with activation energies of 0.74–0.92 eV. He suggested that the center was the B_sV defect. However, the very different levels of the *A* and *B* configurations found in *e*-irradiated material described earlier makes the assignment unlikely. Thus the defect observed by Chantre is probably distinct from the B_sV center discussed here.

II. METHOD

In order to investigate these assignments, calculations were performed using the spin-polarized density functional theory (DFT)[9] together with Hartwigsen, Goedecker, and Hutter pseudopotentials[10] and the AIMPRO[11] code which employs the local density approximation and uses Gaussian basis set orbitals. Details of the method have been given previously.[11] A Monkhorst-Pack (MP) sampling scheme of $2\times2\times2$ *k* points[12] was used for all except for the very largest supercells which are discussed later. Electrical levels were calculated from a comparison of the ionization energies or electron affinities, $E(\pm)-E(0)$, with similar quantities found for a suitable marker having experimentally known electrical levels. This procedure is described in more detail in Ref. 13. We compare the calculated ionization energies and electron affinities of the two defects and then predict the donor and acceptor levels of say B_sV from those of the marker. Thus if the ionization energy of B_sV is 0.1 eV more than that of the marker, it means that it requires 0.1 eV more energy to ionize the defect than the marker and so the donor level of the defect is 0.1 eV below that of the marker. The method works best when a marker is used with levels and charge density close to those of the defect under consideration. For B_sV, VOH was used as a marker while the divacancy was used as a marker for B_sV_2. It is important to note that if the barrier between different configurations of a defect is large, then the defect can be trapped in a metastable configuration at low temperatures and the level observed by DLTS then corresponds to the energy required to change the charge state of the defect in that configuration without relaxation to a lower energy configuration. This is then a vertical transition on a configuration coordinate diagram and not the thermodynamic electrical level, or transition, which corresponds to transitions between global minima in the configuration energy surfaces of different charge states.

Initial calculations were performed in 64 atom supercells and these were then embedded into 216 atom supercells, the largest practical size, and rerelaxed. To check convergence with supercell size several calculations were performed in 512 atom supercells using a minimal basis set. In this case, since a large 512 atom supercell is small in reciprocal space, the Brillouin zone was sampled only at one *k*-point $\pi/4a(111)$, close to the Γ point. The vacancy in Si is known to be a particularly challenging problem for supercell DFT due to the strong defect-defect interactions between neighboring supercells which can induce a large dispersion of deep levels and restrict the ionic relaxation. This is coupled to the problem that the energy surface in configuration space is rather flat and, hence, it is computationally demanding to find the energy minimum with respect to ionic positions in the supercell. It seems, however, that, for the vacancy, the calculated electrical levels converge rapidly with supercell size.[14] Hence, we expect a similar trend for the boron-vacancy defect.

III. RESULTS

A. The boron-vacancy center

The second nearest neighbor B_sV defect, denoted by $2nn(C_1)$, as proposed by Watkins [Fig. 1(i)], was first studied. Atoms *b* and *c* are found to form a weak reconstructed bond of length 2.95 Å in the paramagnetic neutral charge state. This is ~25% longer than the calculated bulk silicon bond length (2.34 Å) but considerably shorter than the calculated separation of atoms equivalent to *b* and *c* in bulk silicon (3.81 Å). A Mulliken population analysis was carried out as described in Ref. 15. It revealed that the spin density

TABLE I. The *s* and *p*-Mulliken populations of the highest occupied Kohn-Sham orbital associated with the $2nn(C_1)$ configuration of B_sV (Fig. 1) compared with experimental EPR and ENDOR results on Si-*G*10 (in parentheses) (see Refs. 2 and 3). The letter given in the "atom" column corresponds to the labeling of Fig. 1. A small *d* component is not included.

Tensor	Atom	*s*-like fraction	*p*-like fraction	Degree of localization (%)
Si-1	*d*	0.143 (0.130)	0.864 (0.870)	20.44 (54.83)
Si-2	*b*/*c*	0.248 (0.281)	0.667 (0.719)	5.02 (5.12)
Si-3	*c*/*b*	0.254 (0.282)	0.630 (0.718)	4.17 (4.79)

of the neutral defect is localized mainly on atom *d* in Fig. 1(*i*). This is in agreement with an analysis of the hyperfine interactions exhibited by *G*10.[2,3] We find only 0.59% of the spin density to be located on the boron atom compared with 20.4% on atom *d*. Table I shows reasonable agreement between the calculated and observed spin localizations and *s*/*p*-like fractions, thus providing further evidence that the Si-*G*10 EPR center is indeed due to a B_sV complex in the configuration proposed by Watkins. The calculated relative populations are not as large as the experimental ones, possibly indicating that the degree of reconstruction between the dangling bonds on atoms *c* and *b* is underestimated by supercell DFT.

The bistability of this center requires other stable configurations of B_sV to be studied. Table II shows the relative stabilities of the configurations of B_sV considered here, the first to fourth nearest neighbor configurations being denoted by 1*nn* to 4*nn*. These configurations are described by Fig. 2. The 1*nn* configuration of B_sV is found to be high in energy in all charge states studied (single positive, neutral, and single negative). We suppose this is because sp^2 bonded boron is a relatively high energy hybridization state compared with sp^3 bonded boron. In the positive charge state the $2nn(C_1)$ configuration was found to be the joint lowest energy structure with the $2nn(C_{1h})$ configuration where they differ only by the pair of atoms sharing a reconstructed bond. They are ~0.1 eV lower in energy than either the 1*nn* or 3*nn* configurations. For the neutral case, which corresponds to the paramagnetic form, the $2nn(C_1)$ configuration is more stable than the others but the difference with the $2nn(C_{1h})$ configuration is very small. Thus the theory is consistent with the assignment of *G*10 to the $2nn(C_1)$ configuration. In the negative charge state, it is the 3*nn* configuration that is found to be the ground state structure by only ~0.06 eV. The 3*nn* structure is found to be marginally (0.08 eV) lower in energy than 4*nn* in the negative charge state, suggesting that 3*nn* is indeed the ground-state configuration in the negative charge state. Thus the calculations support the idea of a boron-vacancy complex assuming different configurations for different Fermi-level positions. However, as we shall now describe, we believe the $2nn(C_{1h})$ configuration is actually higher in energy than the $2nn(C_1)$ configuration but by less than about 0.03 eV in the positive charge state, and with a greater energy difference in the neutral charge state. The closeness of these energies in the positive charge state reflects a weaker reconstruction of the bond between atoms *b* and *c* in Fig. 2 in that charge state.

We now investigate the vertical electrical levels of the defects. These are found as described earlier in 216 atom cells and given in Table II. Although all the structures have deep acceptor levels, these lie in the middle of the gap. In principle such levels are accessible by minority carrier transient spectroscopy but none have been reported, possibly because they are very deep. However, the $2nn(C_1)$ and $2nn(C_{1h})$ configurations have vertical donor levels calculated to lie at $E_v+0.21$ and $E_v+0.24$ eV, respectively, and close to the observed levels.

Suppose that under reverse bias the defect is negatively charged and assumes the 3*nn* configuration which is maintained when the material is quenched to low temperature at that bias. This is then identified with the *B* configuration. After removing the bias at low temperatures, the defect becomes positively charged and has a tendency to move to the $2nn(C_1)$ configuration. However, this requires the vacancy to move closer to boron and the barrier to vacancy motion prevents this from happening at ~62 *K*—the temperature at which the $E_v+0.11$ eV level is monitored by DLTS. Thus this donor level is identified with a vertical transition of the 3*nn* configuration and is in excellent agreement with the calculated vertical donor level of $E_v+0.13$ eV.

Consider now the result of a cool down at zero bias. This results in the defect being positively charged and in the $2nn(C_1)$ or $2nn(C_{1h})$ configurations identified as *A*. The former is the same configuration found in EPR studies carried out at 20 K. At the temperature at which the DLTS is carried out, ~140–200 K,[4] the defect would be present in *both* the $2nn(C_1)$ and $2nn(C_{1h})$ configurations if the energy

TABLE II. The relative energies of the configurations 1*nn*–4*nn* (see Fig. 2) for B_sV and their corresponding vertical electrical levels. The formation energies are given relative to the most stable defect in each charge state. Values in parentheses were calculated in 512 atom supercells while all others are from supercells of 216 atoms. All energies are given in electron-volts.

	$E(-1)$	$E(0)$	$E(+1)$	$E(0/+)$	$E(-/0)$
1*nn*	0.352	0.180	0.135	$E_v+0.26$	$E_c-0.45$
$2nn(C_1)$	0.062 (0.075)	0 (0)	0 (0)	$E_v+0.21$	$E_c-0.56$
$2nn(C_{1h})$	0.220	0.032	0 (0.000)	$E_v+0.24$	$E_c-0.43$
3*nn*	0 (0)	0.042 (0.088)	0.121 (0.227)	$E_v+0.13$	$E_c-0.66$
4*nn*	0.083	0.130	0.201	$E_v+0.14$	$E_c-0.67$

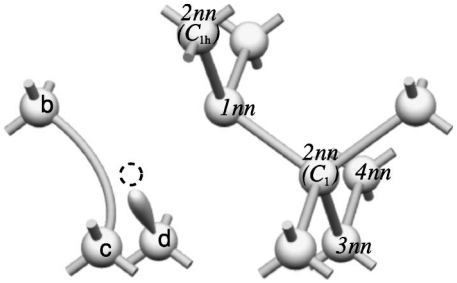

FIG. 2. A piece of silicon showing the vacancy (dashed ring) and the location of the boron atom in the first, 1*nn*, to fourth, 4*nn*, nearest neighbor configurations. The letters correspond to the labeling of Fig. 1 for the $2nn(C_1)$ configuration. Note that the bond reconstruction between *b* and *c* makes the $2nn(C_1)$ and $2nn(C_{1h})$ configurations inequivalent.

difference is around 0.03 eV. The donor level of $2nn(C_1)$ is then identified with the observed $E_v+0.31$ eV level which is close to that calculated at $E_v+0.21$ eV. From Table II, the calculated vertical donor level of $2nn(C_{1h})$ is seen to be $\sim$0.02 eV higher and in reasonable agreement with the experimental value of $E_v+0.37$ eV.

We note that this explanation differs from that of Ref. 4 as now the *two* donor levels of the *A* configuration are identified with two different, and almost degenerate, configurations of the positively charged defect.

B. The boron divacancy B_sV_2 center

Three different B_sV_2 complexes have been considered here. These are the first (1*nn*), second (2*nn*), and fifth nearest neighbor (5*nn*) configurations shown in Fig. 3. These were chosen somewhat arbitrarily since they are the configurations formed when substitutional boron and the divacancy are separated along $\langle 110 \rangle$, but they should demonstrate any trend in the variation of the electrical levels of B_sV_2 with separation.

Of the three configurations it was found that the 2*nn* configuration of B_sV_2 is the most stable in all charge states considered, by $\sim$0.1–0.2 eV. This configuration is shown in Fig. 3(c). The binding energy between boron and the divacancy in B_sV_2 can be obtained by separating the two constituents in a large supercell and is given by the energy difference between the ground-state configuration and the energy asymptotically reached with increasing separation. Such an approach is believed to be more accurate than comparing the formation energies of complexes which become charged when separated. Separating substitutional boron and a divacancy in a neutral 216 atom supercell results in an increase in total energy of just over 0.2 eV indicating a binding energy of this magnitude.

Assuming equilibrium between V_2 and B_s, with V_2 being the minority species, the concentration of V_2-B_s complexes is expected to be given by

$$\frac{N_{V_2} N_B}{N_B + \frac{1}{2} N_{Si} \exp(-E_b/kT)}, \tag{1}$$

where N_{V_2}, N_B, and N_{Si} are the densities of V_2, B, and Si, respectively, E_b is the binding energy of B_s and V_2, k is Boltzmann's constant, and T is temperature. For $N_B \sim 10^{15}$ cm^{-3}, the fraction of V_2 bound to B is negligible above about 140 K. Since low temperature *e* irradiation produces vacancies which become mobile in *p*-type Si only near 200 K, the possibility of creating V_2-B defects seems limited. On the other hand, for heavily doped material when $N_B \sim 10^{19}$ cm^{-3}, the equation above shows appreciable concentrations of B_sV_2 defects can exist up to about 320 K.

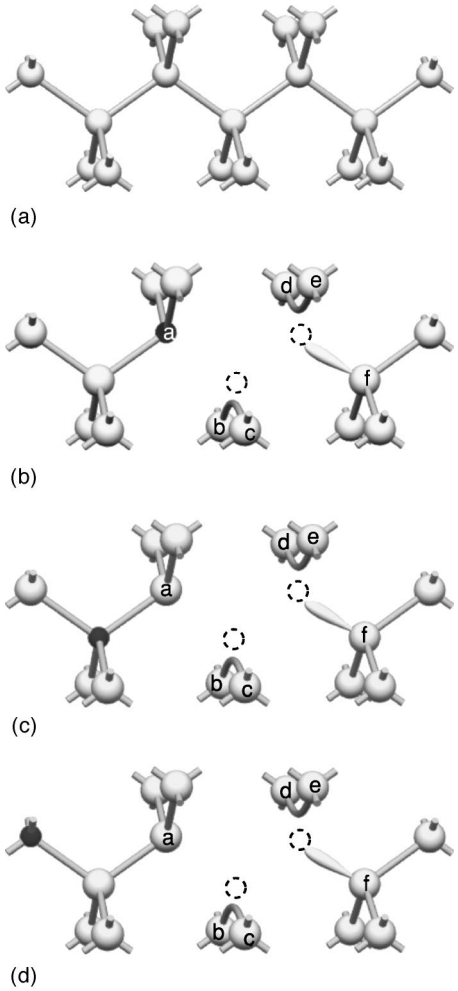

FIG. 3. The three structures of B_sV_2 considered. Part (b) is the 1*nn* configuration, (c) 2*nn*, and (d) 5*nn*. Part (a) shows the equivalent piece of bulk material. Vacancies are represented by dashed rings, black balls are boron and other atoms are silicon. Just as for the divacancy, the dangling bonds left on atoms *b* and *c* and on atoms *d* and *e* reconstruct as shown in the figures.

If B_sV_2 defects are created, then we can estimate the temperature at which they dissociate as follows. The migration energy of V_2 is $\sim$1.3 eV[16] and assuming that B_sV_2 dissociates at a rate $10^{13} \exp(-E_A/kT)$ s^{-1}, where E_A is the activation energy for dissociation given approximately by the sum of the binding energy of B_s and V_2 and the migration energy of the divacancy, then B_sV_2 is predicted to dissociate at around 300 °C.

The calculated levels of the B_sV_2 complexes are given in Table III along with the experimental levels of the divacancy

TABLE III. The relative stabilities and calculated levels of the three configurations of B_sV_2 studied. The experimental levels of the divacancy are also given for comparison (see Refs. 17–19). All energies are given in electron-volts.

	$E(-2)$	$E(-1)$	$E(0)$	$E(+1)$	$E(0/+)$	$E(-/0)$	$E(=/-)$
B_sV_2 1*nn*	0.243	0.178	0.130	0.095	$E_v+0.18$	$E_c-0.62$	$E_c-0.14$
B_sV_2 2*nn*	0	0	0	0	$E_v+0.15$	$E_c-0.66$	$E_c-0.20$
B_sV_2 5*nn*	0.037	0.094	0.198	0.278	$E_v+0.07$	$E_c-0.76$	$E_c-0.26$
V_2 Expt.					$E_v+0.19$	$E_c-0.42$	$E_c-0.23$

which was used as the marker defect for their calculation. Figure 4 shows the associated band structures including that of the divacancy. The first thing to note is that the presence of nearest neighbor substitutional boron perturbs the levels of the divacancy by a small amount. However, this perturbation increases with increasing boron-divacancy separation due to the fact that the substitutional boron removes an electron from the divacancy. This is seen clearly in Fig. 4 which compares the band structures of B_sV_2 in its ground state 2*nn* configuration to the band structure of B_s and V_2 in the same supercell but separated from each other and the band structure of V_2 alone. Hence, for an infinite separation it is seen that the $(=/-)$ level of B_sV_2 should be equal to the $(-/0)$ level of the divacancy. Similarly the $(-/0)$ level of B_sV_2 will tend to the $(0/+)$ level of the divacancy.

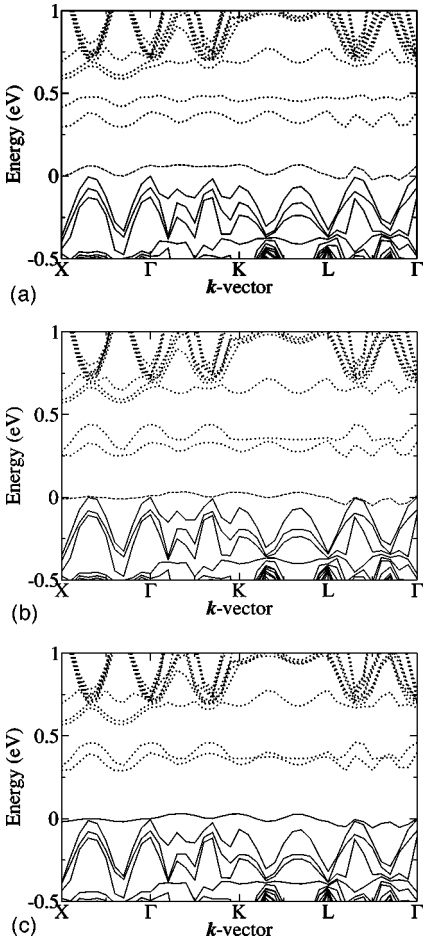

FIG. 4. The band structures of (a) B_sV_2 in the 2*nn* configuration, (b) B_s and V_2 separated within the same supercell, and (c) the divacancy. Solid lines show filled levels, dotted lines are empty levels and the dashed lines show half occupied levels for the neutral defects. As B_s and V_2 are separated the levels of B_sV_2 tend towards those of V_2 but there is one more electron present for the case of V_2.

IV. CONCLUSIONS

In summary, our calculations provide support for the assignment of the Si-*G*10 EPR center to a second nearest neighbor configuration of the B_sV defect. We suppose that this configuration is preferred since boron prefers sp^3 bonding over sp^2 as illustrated in diborane. Furthermore, we have shown, in agreement with experiment, that other configurations have competitive energies and we suggest that the third nearest neighbor configuration is stable in the negative charge state. We assign the $E_v+0.11$ eV level, observed after reverse bias has been applied to the sample during cool down, to a vertical transition associated with this configuration labeled *B*. This configuration is stable in the negative charge state. It is to be noted that this requires the defect to have a suitable acceptor level and we find such a level at about $E_c-0.6$ eV. This level has not been experimentally detected probably because, since it is so deep, it cannot be observed below the temperature of about 260 K at which the defect dissociates. The second nearest neighbor configurations, having C_{1h} and C_1 symmetry due to different bond reconstructions, have almost identical calculated energies but we suggest that the former is actually higher in energy, but by at most 0.03 eV, than the latter in the positive charge state. This energy difference would lead to both configurations being present at temperatures around 140 K, where DLTS was carried out, but not at 20 K where EPR studies were performed. However, we find that a greater energy difference occurs between those two second nearest neighbor configurations in the neutral charge state. Assuming a substantial barrier between those configurations, then this implies that at the temperature of ~140 K used to monitor the $E_v+0.31$ and $E_v+0.37$ eV levels, the defect is found in both configurations that have collectively been labeled *A*, both being in the positive charge state. Thus the two transitions are assigned to the emission of a hole from two different second nearest neighbor configurations.

The smaller energy difference between the configurations

when electrons are removed from the defect is easily understood from the electronic structure of an isolated vacancy.[2] B_sV^+ has the same electronic configuration as a vacancy-boron pair, V^{++}—B_s^-, or $a_1^2t_2^0$. Since there are no electrons in the t_2 manifold, there is no Jahn-Teller distortion resulting in a pairing distortion. Thus the two different second neighbor configurations are degenerate. This is not the case, however, for the neutral and negative charge states when the t_2 manifold becomes occupied and a greater difference in the energies of the structures with dangling bond reconstructions giving C_1 and C_{1h} symmetry is found.

We find that V_2 is only weakly bound with B_s and again the favored configuration involves boron at second nearest neighbor separation from the divacancy. The weak binding implies that these defects are unlikely to be important in Si with low concentrations of B_s although this may not be the case for heavily doped material. The energy levels of B_sV_2 lie close to those of the divacancy.

[1] S. C. Jain, W. Schoenmaker, R. Lindsay, P. A. Stolk, S. Decoutere, M. Willander, and H. E. Maes, J. Appl. Phys. **91**, 8919 (2002).

[2] G. D. Watkins, Phys. Rev. B **13**, 2511 (1976).

[3] M. Sprenger, R. van Kemp, E. G. Sieverts, and C. A. J. Ammerlaan, Phys. Rev. B **35**, 1582 (1987).

[4] S. K. Bains and P. C. Banbury, J. Phys. C **18**, L109 (1985).

[5] C. A. Londos, Phys. Rev. B **34**, 1310 (1986).

[6] N. Zangenberg, J. Goubet, and A. Larsen, Nucl. Instrum. Methods Phys. Res. B **186**, 71 (2002).

[7] S. K. Bains, Ph.D. thesis, University of Reading, United Kingdom, 1985.

[8] A. Chantre, Phys. Rev. B **32**, 3687 (1985).

[9] J. P. Perdew and Y. Wang, Phys. Rev. B **45**, 13 244 (1992).

[10] C. Hartwigsen, S. Goedecker, and J. Hutter, Phys. Rev. B **58**, 3641 (1998).

[11] J. Coutinho, R. Jones, P. R. Briddon, and S. Öberg, Phys. Rev. B **62**, 10 824 (2000).

[12] H. J. Monkhorst and J. D. Pack, Phys. Rev. B **13**, 5188 (1976).

[13] J. Coutinho, V. J. B. Torres, R. Jones, and P. R. Briddon, Phys. Rev. B **67**, 035205 (2003).

[14] M. J. Puska, S. Pöykkö, M. Pesola, and R. M. Nieminen, Phys. Rev. B **58**, 1318 (1998).

[15] R. Jones and P. R. Briddon, *The Ab Initio Cluster Method and the Dynamics of Defects in Semiconductors*, *Semiconductors and Semimetals*, Vol. 51A (Academic Press, Boston, 1998), Chap. 6.

[16] P. Pellegrino, P. Leveque, J. Lalita, A. Hallen, C. Jagadish, and B. G. Svensson, Phys. Rev. B **64**, 195211 (2001).

[17] O. O. Awadelkarim, H. Weman, B. G. Svensson, and J. L. Lindström, J. Appl. Phys. **60**, 1974 (1986).

[18] L. C. Kimerling, *Radiation Effects in Semiconductors* (Institute of Physics, Bristol, 1977), pp. 221, 31.

[19] A. O. Evwaraye and E. Sun, J. Appl. Phys. **47**, 3776 (1976).